Uncaria tomentosa-loaded chitosan oligomers–hydroxyapatite–carbon nitride nanocarriers for postharvest fruit protection

A. Santiago-Aliste, E. Sánchez-Hernández, L. Buzón-Durán, J. L. Marcos-Robles, J. Martín-Gil, and P. Martín-Ramos

SUPPORTING INFORMATION

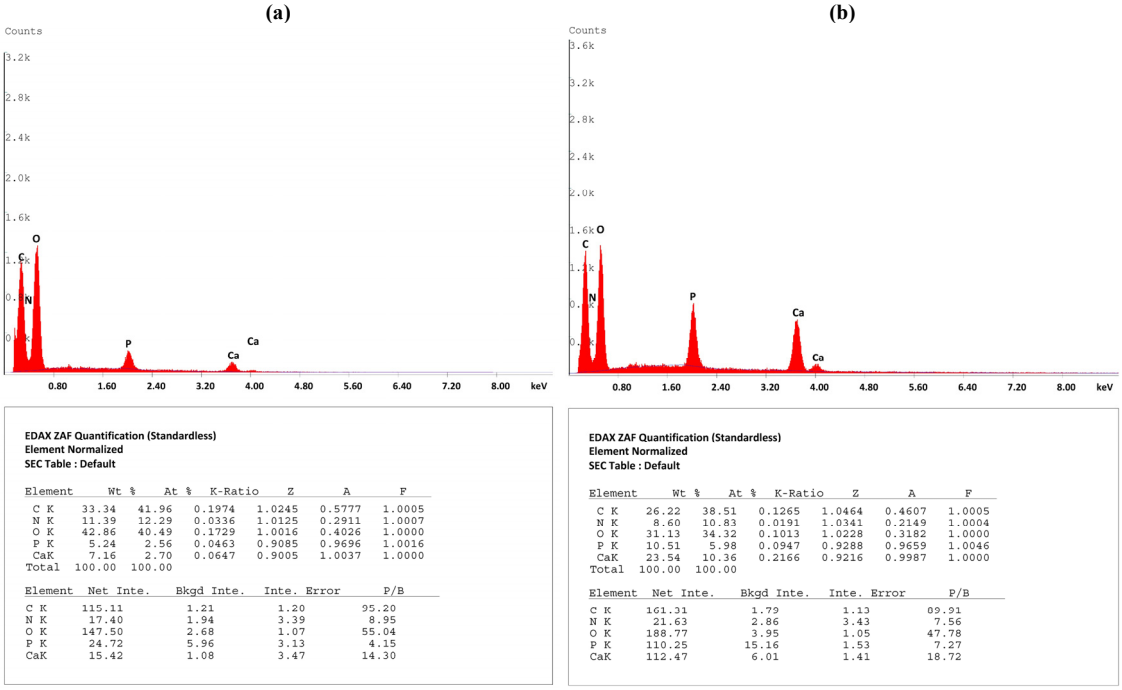

Figure S1. EDS multi-elemental characterization of the (**a**) empty nanocarriers and (**b**) nanocarriers loaded with *U. tomentosa* extract.

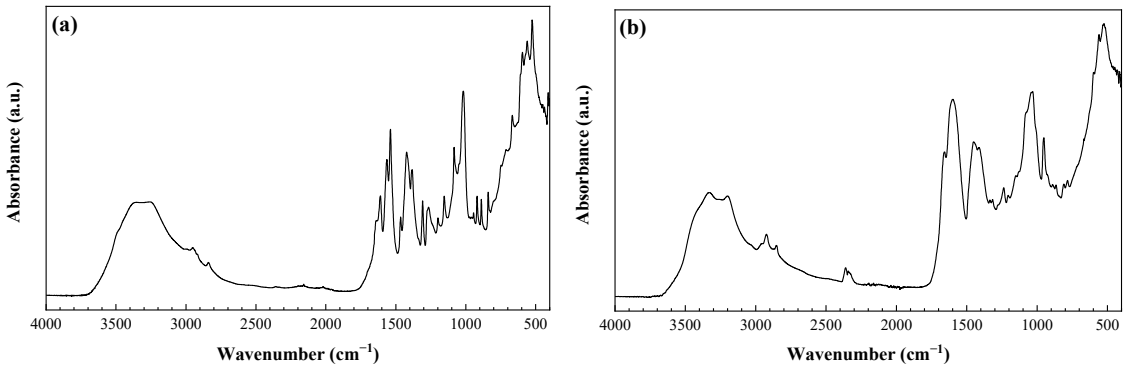

Figure S2. ATR-FTIR spectra of the (**a**) empty nanocarriers and (**b**) nanocarriers loaded with *U. tomentosa* extract.

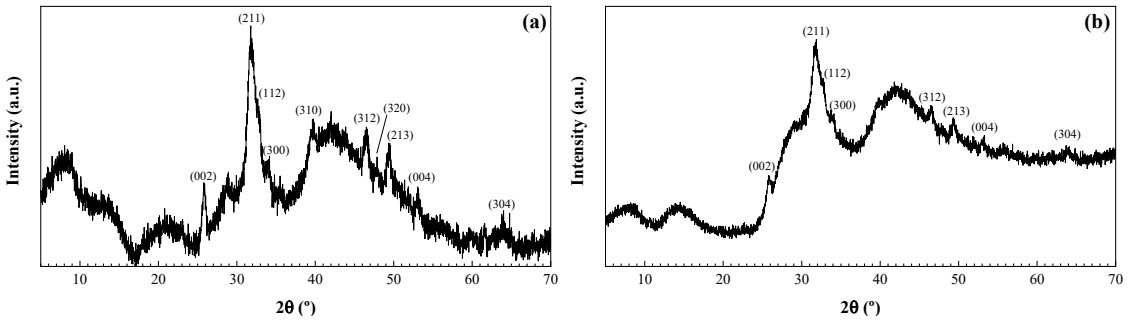

Figure S3. X-ray powder diffraction pattern of the (**a**) empty nanocarriers and (**b**) nanocarriers loaded with *U. tomentosa* extract.

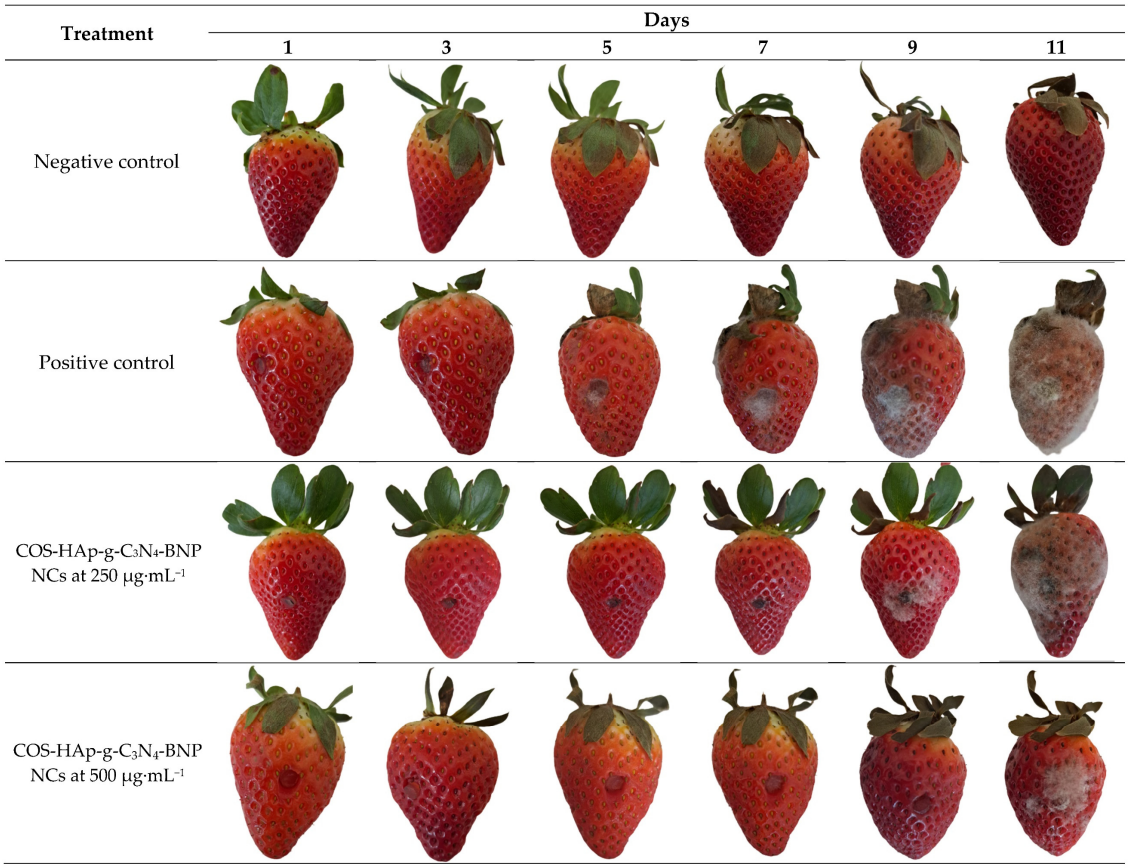

Figure S4. External lesions caused by *B. cinerea* on strawberries cv. "Fortuna" eleven days after artificial inoculation in the presence/absence of the NC-based treatment: (**a**) negative control; (**b**) fruits artificially inoculated with *B. cinerea* (positive control); (**c**) fruits treated with the COS–HAp–g-C_3N_4 NCs loaded with the BNP at 250 µg·mL^{-1}; (**d**) fruits treated with the COS–HAp–g-C_3N_4 NCs loaded with the BNP at 500 µg·mL^{-1}. Only one replicate per treatment is shown.

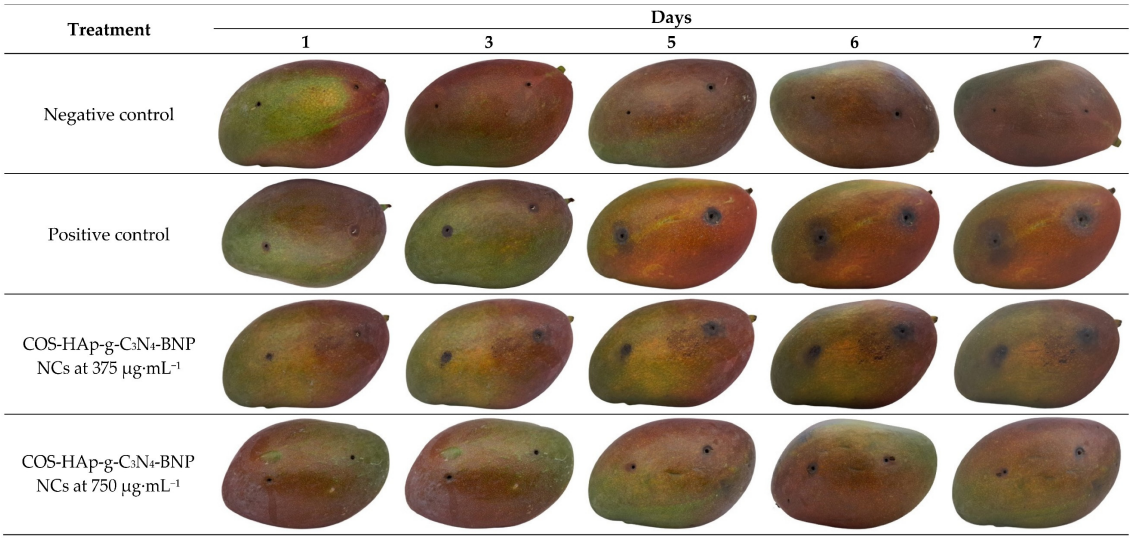

Figure S5. External lesions caused by *C. gloeosporioides* on mangoes cv. "Keitt" seven days after artificial inoculation in the presence/absence of the NC-based treatment: (**a**) negative control; (**b**) fruits artificially inoculated with *C. gloeosporioides* (positive control); (**c**) fruits treated with the COS–HAp–g-C_3N_4 NCs loaded with the BNP at 375 µg·mL^{-1}; (**d**) fruits treated with the COS–HAp–g-C_3N_4 NCs loaded with the BNP at 750 µg·mL^{-1}. Only one replicate per treatment is shown.

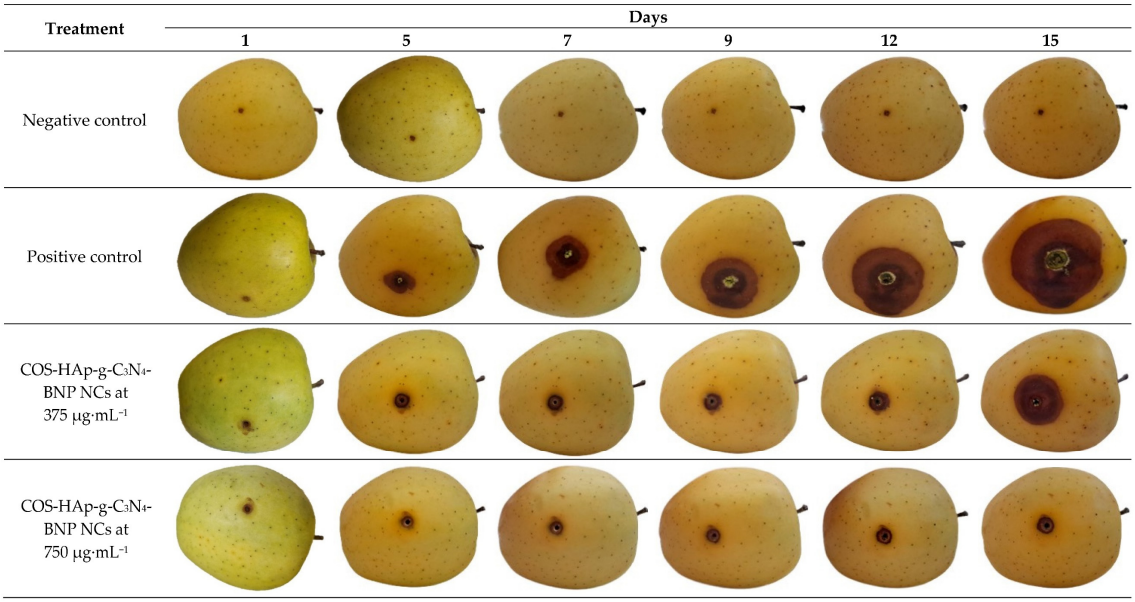

Figure S6. External lesions caused by *P. expansum* on apples cv. "Golden Delicious" fifteen days after artificial inoculation in the presence/absence of the NC-based treatment: (**a**) negative control; (**b**) fruits artificially inoculated with *P. expansum* (positive control); (**c**) fruits treated with the COS–HAp–g-C_3N_4 NCs loaded with the BNP at 375 µg·mL^{-1}; (**d**) fruits treated with the COS–HAp–g-C_3N_4 NCs loaded with the BNP at 750 µg·mL^{-1}. Only one replicate per treatment is shown.

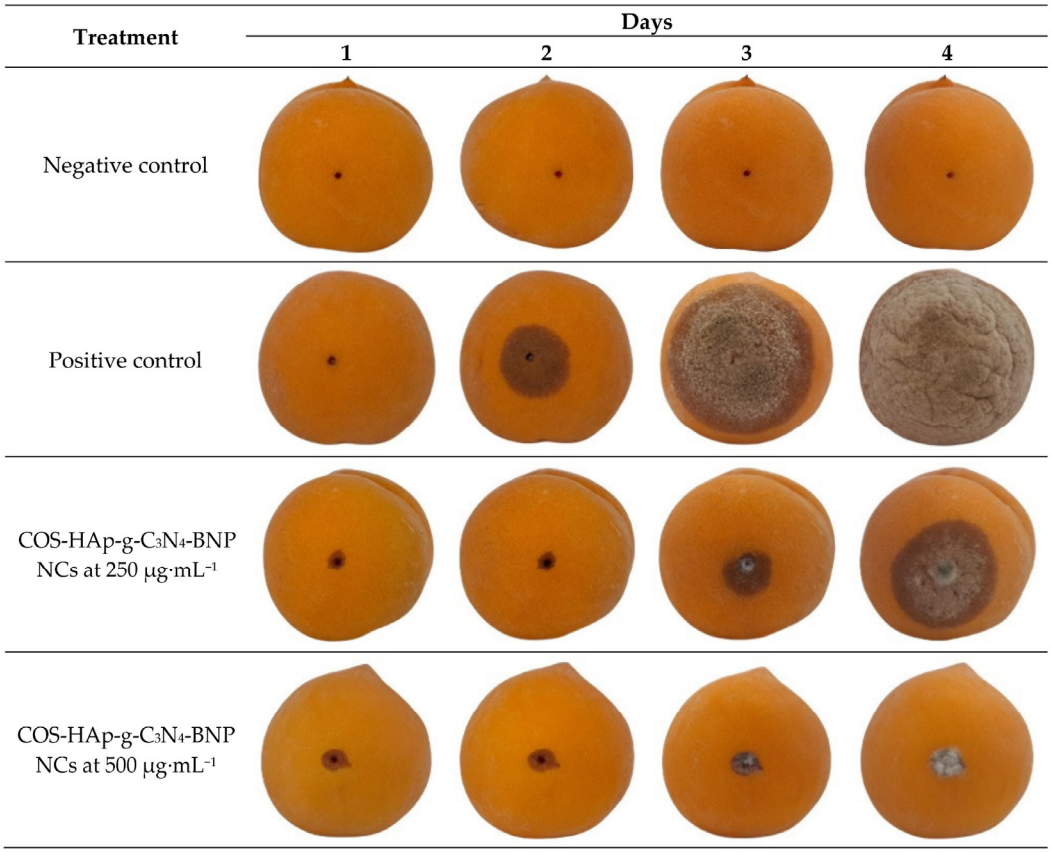

Figure S7. External lesions caused by *M. laxa* on peaches cv. "Summer sun" four days after artificial inoculation in the presence/absence of the NC-based treatment: (**a**) negative control; (**b**) fruits artificially inoculated with *M. laxa* (positive control); (**c**) fruits treated with the COS–HAp–g-C_3N_4 NCs loaded with the BNP at 250 μg·mL^{-1}; (**d**) fruits treated with the COS–HAp–g-C_3N_4 NCs loaded with the BNP at 500 μg·mL^{-1}. Only one replicate per treatment is shown.

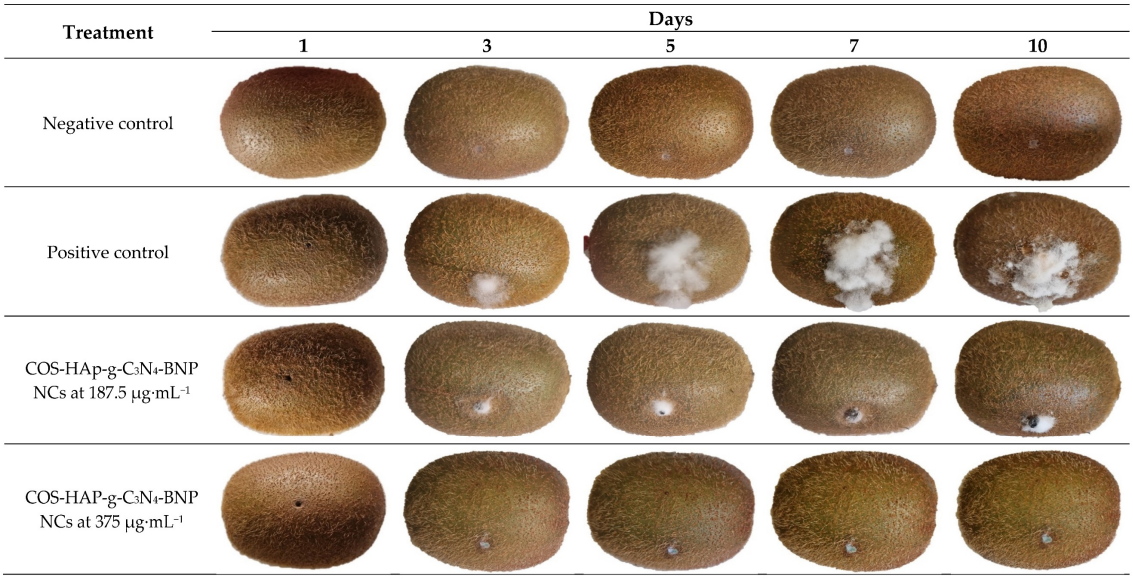

Figure S8. External lesions caused by *S. sclerotiorum* on kiwifruit cv. "Hayward Green" ten days after artificial inoculation in the presence/absence of the NC-based treatment: (**a**) negative control; (**b**) fruits artificially inoculated with *S. sclerotiorum* (positive control); (**c**) fruits treated with the COS–HAp–g-C_3N_4 NCs loaded with the BNP at 187.5 μg·mL^{-1}; (**d**) fruits treated with the COS–HAp–g-C_3N_4 NCs loaded with the BNP at 375 μg·mL^{-1}. Only one replicate per treatment is shown.

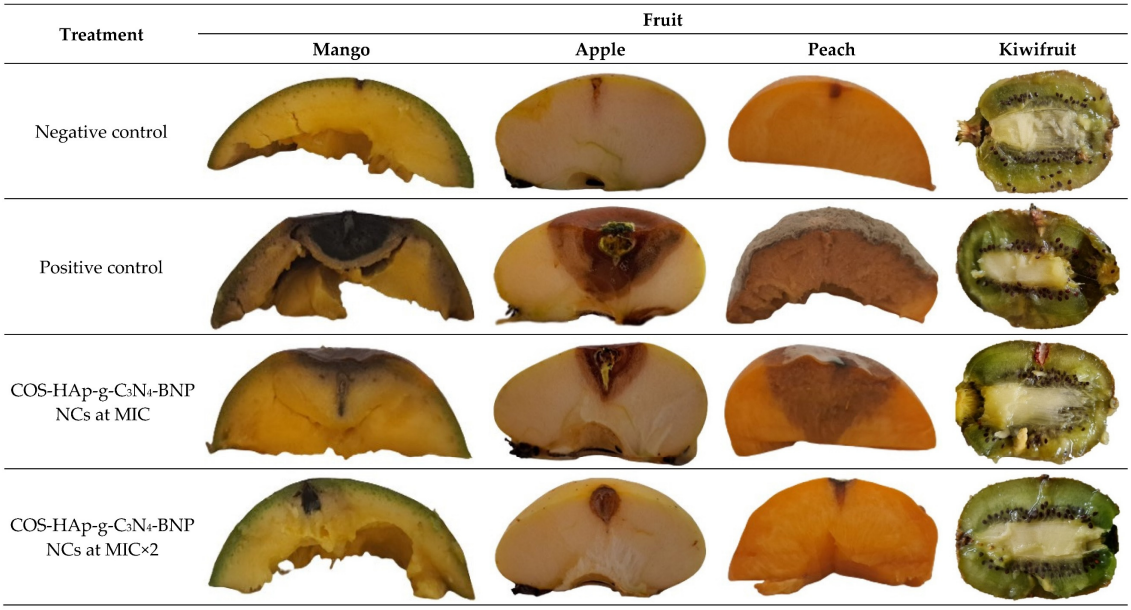

Figure S9. Internal lesions caused by *C. gloeosporioides* on mangoes, *P. expansum* on apples, *M. laxa* on peaches, and *S. sclerotiorum* on kiwifruit in the presence/absence of the NC-based treatment. Only one replicate per treatment is shown.

Table S1. Results of the normality and homoscedasticity tests, along with those of Kruskal-Wallis test, for the mycelial growth inhibition data presented in Figure 2 of the main document.

	B. cinerea	***C. gloeosporioides***	***P. expansum***	***M. laxa***	***S. sclerotiorum***
Test on the normality of the residues (p-value, two-tailed) *	<0.0001	<0.0001	<0.0001	<0.0001	<0.0001
Test for homoscedasticity of the residuals, treatment*concentration factor (p-value, two-tailed) *	<0.0001	<0.0001	<0.0001	<0.0001	< 0.0001
Kruskal-Wallis test (p-value, one-tailed)	<0.0001	<0.0001	<0.0001	<0.0001	<0.0001

Since the computed p-values are lower than the significance level $\alpha = 0.05$, one can reject the null hypothesis (i.e., that the residuals follow a Normal distribution in the case of the Shapiro-Wilk test and that the residuals are homoscedastic in the case of Levene test)

Table S2. Results of the ANOVA, normality, and homoscedasticity tests for the lesion size data presented in Table 4 of the main document.

	Strawberry	**Mango**	**Apple**	**Peach**	**Kiwifruit**
Analysis of variance (Pr > F)	<0.0001	<0.0001	<0.0001	<0.0001	<0.0001
Test on the normality of the residues (p-value, two-tailed) *	0.365	0.371	0.294	0.386	0.136
Test for homoscedasticity of the residuals (p-value, two-tailed) *	0.212	0.217	0.274	0.228	0.115

Since the computed p-values are greater than the significance level $\alpha = 0.05$, one cannot reject the null hypothesis (i.e., that the residuals follow a Normal distribution in the case of the Shapiro-Wilk test and that the residuals are homoscedastic in the case of Levene test)

Table S3. Kruskal-Wallis test and multiple pairwise comparisons using the Conover-Iman procedure for *B. cinerea* mycelial growth inhibition values.

Treatment|Concentration	Mean of ranks	Groups
COS–HAp–g-C_3N_4|1000	23.000	A
COS–HAp–g-C_3N_4|1500	23.000	A
COS–HAp–g-C_3N_4|500	23.000	A
COS–HAp–g-C_3N_4|750	23.000	A
COS–HAp–g-C_3N_4–BNP|1000	23.000	A
COS–HAp–g-C_3N_4–BNP|1500	23.000	A
COS–HAp–g-C_3N_4–BNP|250	23.000	A
COS–HAp–g-C_3N_4–BNP|375	23.000	A
COS–HAp–g-C_3N_4–BNP|500	23.000	A
COS–HAp–g-C_3N_4–BNP|750	23.000	A
U. tomentosa|1000	23.000	A
U. tomentosa|1500	23.000	A
U. tomentosa|375	23.000	A
U. tomentosa|500	23.000	A
U. tomentosa|750	23.000	A
COS–HAp–g-C_3N_4–BNP|187.5	47.000	B
U. tomentosa|250	50.000	C
U. tomentosa|187.5	53.000	D
U. tomentosa|125	56.000	E
U. tomentosa|93.75	59.167	F
COS–HAp–g-C_3N_4|375	61.833	G
COS–HAp–g-C_3N_4–BNP|125	65.000	H
U. tomentosa|62.5	68.000	I
COS–HAp–g-C_3N_4|250	71.000	J
COS–HAp–g-C_3N_4–BNP|93.75	74.000	K
COS–HAp–g-C_3N_4–BNP|62.5	77.000	L
COS–HAp–g-C_3N_4|125	86.000	M
COS–HAp–g-C_3N_4|187.5	86.000	M
COS–HAp–g-C_3N_4|62.5	86.000	M
COS–HAp–g-C_3N_4|93.75	86.000	M
Control|0	86.000	M

Treatments/controls labeled with the same letters are not significantly different at $p < 0.05$.

Table S4. Kruskal-Wallis test and multiple pairwise comparisons using the Conover-Iman procedure for *C. gloeosporioides* mycelial growth inhibition values.

Treatment|Concentration	Mean of ranks	Groups											
COS–HAp–g-C_3N_4|1000	17.000	A											
COS–HAp–g-C_3N_4|1500	17.000	A											
COS–HAp–g-C_3N_4|500	17.000	A											
COS–HAp–g-C_3N_4|750	17.000	A											
COS–HAp–g-C_3N_4–BNP|1000	17.000	A											
COS–HAp–g-C_3N_4–BNP|1500	17.000	A											
COS–HAp–g-C_3N_4–BNP|375	17.000	A											
COS–HAp–g-C_3N_4–BNP|500	17.000	A											
COS–HAp–g-C_3N_4–BNP|750	17.000	A											
U. tomentosa|1000	17.000	A											
U. tomentosa|1500	17.000	A											
COS–HAp–g-C_3N_4|375	35.000		B										
COS–HAp–g-C_3N_4–BNP|250	38.000		B	C									
U. tomentosa|750	41.000			C	D								
COS–HAp–g-C_3N_4–BNP|187.5	44.000				D	E							
U. tomentosa|500	47.167					E	F						
COS–HAp–g-C_3N_4|250	49.833						F	G					
COS–HAp–g-C_3N_4|187.5	54.833							G	H				
U. tomentosa|375	54.833							G	H				
COS–HAp–g-C_3N_4–BNP|125	59.333								H	I			
COS–HAp–g-C_3N_4|125	63.167									I	J		
U. tomentosa|250	64.333									I	J		
COS–HAp–g-C_3N_4–BNP|93.75	68.333										J	K	
U. tomentosa|125	71.167											K	
U. tomentosa|187.5	72.000											K	
COS–HAp–g-C_3N_4|62.5	84.500												L
COS–HAp–g-C_3N_4|93.75	84.500												L
COS–HAp–g-C_3N_4–BNP|62.5	84.500												L
Control|0	84.500												L
U. tomentosa|62.5	84.500												L
U. tomentosa|93.75	84.500												L

Treatments/controls labeled with the same letters are not significantly different at $p < 0.05$.

Table S5. Kruskal-Wallis test and multiple pairwise comparisons using the Conover-Iman procedure for *M. laxa* mycelial growth inhibition values.

Treatment|Concentration	Mean of ranks	Groups
COS–HAp–g-C_3N_4|1000	15.500	A
COS–HAp–g-C_3N_4|1500	15.500	A
COS–HAp–g-C_3N_4|750	15.500	A
COS–HAp–g-C_3N_4–BNP|1000	15.500	A
COS–HAp–g-C_3N_4–BNP|1500	15.500	A
COS–HAp–g-C_3N_4–BNP|250	15.500	A
COS–HAp–g-C_3N_4–BNP|375	15.500	A
COS–HAp–g-C_3N_4–BNP|500	15.500	A
COS–HAp–g-C_3N_4–BNP|750	15.500	A
U. tomentosa|1500	15.500	A
COS–HAp–g-C_3N_4|500	32.333	B
U. tomentosa|1000	34.667	B C
U. tomentosa|750	38.333	C D
COS–HAp–g-C_3N_4–BNP|187.5	41.000	D E
COS–HAp–g-C_3N_4|375	43.833	D E
COS–HAp–g-C_3N_4–BNP|125	46.833	E F
U. tomentosa|500	50.000	F G
COS–HAp–g-C_3N_4|250	53.000	G H
U. tomentosa|375	56.000	H I
COS–HAp–g-C_3N_4|187.5	59.667	I J
COS–HAp–g-C_3N_4|–BNP|93.75	65.167	J K
U. tomentosa|250	65.167	J K
COS–HAp–g-C_3N_4|125	69.667	K
COS–HAp–g-C_3N_4–BNP|62.5	69.667	K
U. tomentosa|187.5	69.667	K
U. tomentosa|125	77.000	L
COS–HAp–g-C_3N_4|62.5	86.000	M
COS–HAp–g-C_3N_4|93.75	86.000	M
Control|0	86.000	M
U. tomentosa|62.5	86.000	M
U. tomentosa|93.75	86.000	M

Treatments/controls labeled with the same letters are not significantly different at $p < 0.05$.

Table S6. Kruskal-Wallis test and multiple pairwise comparisons using the Conover-Iman procedure for *P. expansum* mycelial growth inhibition values.

Treatment|Concentration	Mean of ranks	Groups
COS–HAp–g-C_3N_4|1000	12.500	A
COS–HAp–g-C_3N_4|1500	12.500	A
COS–HAp–g-C_3N_4–BNP|1000	12.500	A
COS–HAp–g-C_3N_4–BNP|1500	12.500	A
COS–HAp–g-C_3N_4–BNP|375	12.500	A
COS–HAp–g-C_3N_4–BNP|500	12.500	A
COS–HAp–g-C_3N_4–BNP|750	12.500	A
U. tomentosa|1500	12.500	A
COS–HAp–g-C_3N_4–BNP|250	26.000	B
U. tomentosa|1000	29.667	B C
COS–HAp–g-C_3N_4|750	31.667	B C
U. tomentosa|750	36.667	B C D
U. tomentosa|500	38.500	C D
COS–HAp–g-C_3N_4|500	39.833	C D E
COS–HAp–g-C_3N_4|375	47.000	D E F
U. tomentosa|375	47.000	D E F
COS–HAp–g-C_3N_4–BNP|187.5	50.667	E F G
COS–HAp–g-C_3N_4|250	51.167	F G
COS–HAp–g-C_3N_4|187.5	56.167	F G H
U. tomentosa|250	57.333	F G H
U. tomentosa|187.5	60.667	G H
U. tomentosa|125	66.000	H I
COS–HAp–g-C_3N_4|125	67.000	H I
COS–HAp–g-C_3N_4|93.75	74.333	I J
COS–HAp–g-C_3N_4–BNP|125	79.333	J
COS–HAp–g-C_3N_4|62.5	83.000	J
COS–HAp–g-C_3N_4–BNP|62.5	83.000	J
COS–HAp–g-C_3N_4–BNP|93.75	83.000	J
Control|0	83.000	J
U. tomentosa|62.5	83.000	J
U. tomentosa|93.75	83.000	J

Treatments/controls labeled with the same letters are not significantly different at $p < 0.05$.

Table S7. Kruskal-Wallis test and multiple pairwise comparisons using the Conover-Iman procedure for *S. sclerotiorum* mycelial growth inhibition values.

Treatment|concentration	Mean of ranks	Groups
COS–HAp–g-C_3N_4|1000	23.000	A
COS–HAp–g-C_3N_4|1500	23.000	A
COS–HAp–g-C_3N_4|500	23.000	A
COS–HAp–g-C_3N_4|750	23.000	A
COS–HAp–g-C_3N_4–BNP|1000	23.000	A
COS–HAp–g-C_3N_4–BNP|1500	23.000	A
COS–HAp–g-C_3N_4–BNP|187.5	23.000	A
COS–HAp–g-C_3N_4–BNP|250	23.000	A
COS–HAp–g-C_3N_4–BNP|375	23.000	A
COS–HAp–g-C_3N_4–BNP|500	23.000	A
COS–HAp–g-C_3N_4–BNP|750	23.000	A
U. tomentosa|1000	23.000	A
U. tomentosa|1500	23.000	A
U. tomentosa|500	23.000	A
U. tomentosa|750	23.000	A
COS–HAp–g-C_3N_4|375	47.000	B
U. tomentosa|375	50.000	C
COS–HAp–g-C_3N_4–BNP|125	53.000	D
U. tomentosa|250	56.000	E
COS–HAp–g-C_3N_4|125	75.500	F
COS–HAp–g-C_3N_4|187.5	75.500	F
COS–HAp–g-C_3N_4|250	75.500	F
COS–HAp–g-C_3N_4|62.5	75.500	F
COS–HAp–g-C_3N_4|93.75	75.500	F
COS–HAp–g-C_3N_4–BNP|62.5	75.500	F
COS–HAp–g-C_3N_4–BNP|93.75	75.500	F
Control|0	75.500	F
U. tomentosa|125	75.500	F
U. tomentosa|187.5	75.500	F
U. tomentosa|62.5	75.500	F
U. tomentosa|93.75	75.500	F

Treatments/controls labeled with the same letters are not significantly different at $p < 0.05$.

Table S8. Nanocarriers reported in the literature for the control of *Botrytis cinerea*, *Colletotrichum* spp., *Monilinia* spp., *Penicillium* spp., and *Sclerotinia sclerotiorum*.

Phytopathogen	Type of Nanocarrier	Active Ingredient Encapsulated	Encapsulation Efficiency	Type of Bioassay	Activity	Ref.
	Quaternary ammonium salt modified-mesoporous silica NPs modified with carboxylatopillar[5]arene capping	Berberine hydrochloride	n.a.	In vitro, ex-situ, and in vivo	In vitro: 36.20 and 48.36% at 60 and 120 μg·mL^{-1}, respectively. Ex-situ (detached tomato leaves): 45.47 and 52.71% at 60 and 120 μg·mL^{-1}, respectively, after 54 h. In vivo (potted tomato leaves): high inhibition.	[1]
	Poly (lactic-co-glycolic acid) NPs	Pterostilbene	37-75%	In vitro	In vitro: 25% at 20 μg·mL^{-1} after 72 h.	[2]
	β-Glucans and/or soy lecithin	Resveratrol	67-94%	In vitro	In vitro: 50-70% inhibition at 100 μg·mL^{-1}	[3]
	β-Cyclodextrin (CD) inclusion compounds dispersed in a low-density polyethylene (LDPE) film	Carvacrol and trans-cinnamaldehyde	61-92%	In vitro	In vitro: 31.4 and 10.9% fungicidal activity for LDPE doped with 1 wt% of β-CD-carvacrol or β-CD-cinnamaldehyde, respectively.	[4]
	Chitosan NPs	D-limonene	89.4-92.3%	In vivo	In vivo: activation of plant (*Arabidopsis thaliana*) immune response @ chitosan 250 μg·mL^{-1} and D-limonene 5 mg·mL^{-1} dose.	[5]
	Mesoporous silica NPs	Eugenol (encapsulated) and Ag^{+} (coordinated to polydopamine as a coating)	n.a.	In vitro, ex-situ, and in vivo	In vitro: 47.92% and 71.38% inhibition at 30 and 60 μg·mL$^{-1,}$ respectively. Ex situ (detached tomato leaves): 72.59% and 82.63% at 60 and 120 μg·mL^{-1}, respectively. In vivo (potted tomato leaves): high protection at both doses.	[6]
	Casein NPs	Eugenol	67.1-90.4%	In vitro and ex-situ	In vitro: MIC = 40.2 μg·mL^{-1} of eugenol. Ex-situ (pear fruit): 23 and 45% disease incidence after 8 and 12 days, respectively.	[7]
	ZnO@OAm nanorod-based nanocapsules	Geraniol	33-78%	In vitro and in vivo	In vitro: EC_{50} = 150 μg·mL^{-1} for 1:3 ZnO:geraniol ratio. In vivo (tomato and cucumber plants): disease index of 3 (vs. 6 for control) in cucumber and 4 (vs. 7 for control) in tomato after 96 h	[8]
	Chitosan-pea protein	EO from *Hyssopus officinalis*	n.a.	In vitro and ex situ	In vitro: 85% inhibition at 2 mg·mL^{-1}. Ex-situ (strawberry fruits): 12.2% infection on day 8 at 2 mg·mL^{-1}; 0.8 disease severity (vs. 4.3 for control) on day 9.	[9]
	Chitosan NPs	EO from *Pistacia atlantica* hulls	43.3-61.5%	In vitro and ex-situ	In vitro: MIC = 20 μg·mL^{-1}. Ex-situ (strawberry fruits): 23.4% infection on the 10th day at 20 μg mL^{-1}.	[10]
	Poly (vinyl alcohol)/chitosan nanospheres	EO from *Salvia officinalis*	66.1-73.3%	In vitro	In vitro: MIC = 0.16-0.40 μL·mL^{-1} for 0.25%, 0.5%, and 1% *v/v* of sage EO	[11]
	Chitosan	EO from *Zataria multiflora*	3.2-45%	In vitro and ex-situ	In vitro: MIC = 1500 μg·mL^{-1}. Ex-situ (strawberry fruits): 16.67% infection rate on day 9 at 1500 μg·mL^{-1}; 1.5 disease severity (vs. 4.9 for control).	[12]
	Cyclodextrin-based nanosponges	1-methylcyclopropene *	n.a.	Ex-situ	Ex-situ (cut flowers): 40% inhibition at 0.25 μL·L^{-1} after 11 days.	[13]
	Chitosan-gum arabic-coated liposomes	5I-1H-indole *	92%	In vitro and ex-situ	In vitro: MIC = 25 μg·mL^{-1}. Ex-situ (strawberries, Kyoho Japanese grapes, and tangerines): high protection at 200 μg mL^{-1}.	[14]
	ZIF-67 NPs	Boscalid *	18% loading ratio	In vitro and in vivo	In vitro: EC_{90} = 17.6 μg·mL^{-1}. In vivo (citrus leaves): full inhibition at lower dose than non-encapsulated Boscalid.	[15]

	Imidazolate framework-8	Dazomet *	4.4% loading content	In vitro and in vivo	In vitro: EC_{50} = 7.9 μg·mL^{-1}. In vivo (potted cucumber leaves): 75% efficacy after 10 days, higher than that of dazomet (52%).	[16]
B. cinerea, S. sclerotiorum	Fenhexamid and polyhexamethylene biguanide NPs	Fenhexamid *	n.a.	In vitro and in vivo	In vitro: EC_{50} = 3.26 and 0.18 μg·mL^{-1} for *B. cinerea* and *S. sclerotiorum*, respectively. In vivo (tomato and rape for *B. cinerea* and *S. sclerotiorum*, resp.): some protection in both cases at 1700 μg·mL^{-1}	[17]
C. capsici	rGO-decorated $Cu_{2-x}Se$ NCs, coated with chitosan	Captan *	36%	In vitro and in vivo	In vitro: EC_{50} = 200 μg·mL^{-1} at neutral pH. In vivo (chili leaves): 25% disease incidence (vs. 55% for control) after 10 days	[18]
C. gloeosporioides	Glucose oxidase-N-succinyl chitosan nanospheres	Empty	-	In vitro and in vivo	In vitro: EC_{50} = 211.2 μg·mL^{-1}. Ex-situ (mango fruits): high protection at 125 μg·mL^{-1} for 7 days.	[19]
	Chitosan-agar	EO from *Cymbopogon citratus*	83%	In vitro and in vivo	In vitro: MIC = 1370 μg·mL^{-1}. In vivo (Topito chili plants): high protection for 30-40 EO (non-nano) capsules dosage.	[20]
	Polyvinyl alcohol nanofibers	EOs from *Thymus vulgaris* and *Piper betel*	40−76%	In vitro and ex-situ	In vitro: ENF containing 300 μg·mL^{-1} of blended EOs showed 24 mm inhibition zone on 6th day of incubation. Ex-situ (sapota fruits): 40% disease incidence (vs. 100% for control).	[21]
	Benzoylated lignin sulfonates-based NCs	Difenoconazole *	n.a.	In vitro	In vitro: EC_{50} = 0.36 μg·mL^{-1}; 75% inhibition at 4 μg·mL^{-1}. In vivo (strawberry leaves): 82% inhibition after 14 days.	[22]
C. gossypii	Chitosan-lactide copolymer	Pyraclostrobin *	45-92%	In vitro	In vitro: 85.1% inhibition at 15 μg·mL^{-1}.	[23]
C. higginsianum	Poly (lactic acid) microspheres	Azoxystrobin *	78.5-92.7%	In vitro	In vitro: EC_{50} = 2-21.3 μg·mL^{-1} depending on microsphere size.	[24]
C. nymphaeae	Copper NPs	EOs from *Thymus daenensis* and *Anethum graveolens*	n.a.	In vitro	In vitro: EC_{50} = 51.3 and 42.3 μg·mL^{-1} for dill and thyme EOs encapsulated in Cu NPs, respectively.	[25]
M. fructicola	Zein casein NPs	Natamycin *	55-84%	In vitro and ex-situ	In vitro: MIC = 80 μg·mL^{-1}, similar to non-encapsulated natamycin. Ex-situ (peach fruit): higher protection than non-encapsulated natamycin.	[26]
P. citrinum	*Azadirachta indica* oil nanoemulsion in Tween 20 and water	-	-	In vitro	In vitro: 25 mm inhibition zone at 3% *w/v*, comparable to positive control.	[27]
P. fellutenum	Chitosan	EO from *Cymbopogon nardus*	46.7-81.6%	In vitro	In vitro: MIC = 0.16 μL·mL^{-1}.	[28]
P. italicum, P. chrysogenum, P. spinulosum	Chitosan nanomatrix	EO from *Coriandrum sativum*	26.5-78%	In vitro	In vitro: MICs not specified, but higher efficacy was attained for the encapsulated EO in all cases.	[29]
P. notatum	Curcumin NPs	-	-	In vitro	In vitro: no activity (MIC > 1000 μg·mL^{-1})	[30]
	Chitosan	EO from *Cymbopogon commutatus*	19.8-44.8%	In vitro	In vitro: 56.5% inhibition at 5 mg·mL^{-1}.	[31]
P. chrysogenum	Carbomer (Carbopol Aqua SF1) nanogels, with and without poly(diallyldimethylammonium chloride) surface functionalization	Zinc bis(dimethyldithiocarbamate) (Ziram) * and 3-iodo-2-	-	In vitro	In vitro: no inhibition for Ziram-loaded NCs; full inhibition for carbopol 0.1 wt% + IPBC 0.02-0.04 wt% when the NC suspensions were applied in the bulk and the surface of the growth media	[32]

		propynyl-N-butylcarbamate (IPBC) *				
P. digitatum, *P. italicum*	Mesoporous silica-chitosan NPs	Prochloraz *	25.4%	In vivo and ex situ	In vivo (citrus trees): 12.7% infection rate at 400 μg·mL^{-1} (pre-harvest treatment). Ex-situ (citrus fruit, postharvest treatment): disease severity = 3 after 10 days (vs. 5 for control).	[33]
Penicillium spp.	Rod-like hollow silica ($hSiO_2$) with tannic acid-Cu complexes capping	Dinotefuran *	n.a.	In vitro	In vitro: 26.4 and 67.1% inhibition at 100 and 200 μg·mL^{-1}, respectively.	[34]
S. sclerotiorum	Mesoporous selenium functionalized with trimethylammoniumpillar[5]arene and methyl orange	Carbendazim *	23.5% loading rate	In vitro and in vivo	In vitro: EC_{50} = 0.41 μg·mL^{-1}. In vivo (oilseed rape plants): 30.64% lesion area (vs. full infection in control) after 72 h.	[35]
	Disulfide-bridged mesoporous organosilica nanoparticles with calcium carbonate as the capping agent	Prochloraz *	8.9% loading ratio	In vitro and in vivo	In vitro: EC_{50} = 0.142 μg·mL^{-1}. In vivo (potted rapeseed plants): 36.1% efficacy after 7 days.	[36]
	Starch-doped porous $CaCO_3$ with tannic acid-Cu complexes capping	Prochloraz *	15.2% loading capacity	In vitro and in vivo	In vitro: EC_{50} = 0.144 μg·mL^{-1}. In vivo (potted oilseed rape leaves): 56.8% control effect after 7 days for 100 μg·mL^{-1}.	[37]
	Hollow mesoporous silica with tannic acid-Cu as a capping agent	Prochloraz *	17.7% loading	In vitro	In vitro: EC_{50} = 0.131 μg·mL^{-1}; 91.05% inhibition at 0.8 μg·mL^{-1}.	[38]
	Phosphonium ionic liquid-porous hollow silica microcapsules coated with pectin	Prochloraz *	35.95%	In vitro and in vivo	In vitro: 97.9% control efficacy at 0.1 μg·mL^{-1} of encapsulated PRO. In vivo (rapeseed leaves): 97% efficacy after 9 days (vs. 5.8% for non-encapsulated PRO).	[39]
	Zeolitic imidazolate framework-8 NPs	Prochloraz * + 2,4-dinitrobenzaldehyde (pH-jump reagent)	n.a.	In vitro and in vivo	In vitro: EC_{50} = 0.122 μg·mL^{-1}. In vivo (oilseed rape plants): 51.2% efficacy after 14 days.	[40]
	Graphene oxide	Pyraclostrobin *	87.04%	In vitro and in vivo	In vitro: 97% inhibition at 200 μg·mL^{-1}. In vivo (oilseed rape plants): 62.32% control efficacy at 200 μg·mL^{-1} after 7 days.	[41]

EC_{50}: half maximal effective concentration; EO: essential oil; MIC: minimum inhibitory concentration; NC: nanocarrier; NP: nanoparticle; n.a.: no activity; * Conventional fungicides.

References (reference numbers do not match those that appear in the main document)

1. Wang, C.-Y.; Lou, X.-Y.; Cai, Z.; Zhang, M.-Z.; Jia, C.; Qin, J.-C.; Yang, Y.-W. Supramolecular nanoplatform based on mesoporous silica nanocarriers and pillararene nanogates for fungus control. *ACS Applied Materials & Interfaces* **2021**, *13*, 32295-32306, doi:10.1021/acsami.1c08582.
2. De Angelis, G.; Simonetti, G.; Chronopoulou, L.; Orekhova, A.; Badiali, C.; Petruccelli, V.; Portoghesi, F.; D'Angeli, S.; Brasili, E.; Pasqua, G.; Palocci, C. A novel approach to control *Botrytis cinerea* fungal infections: uptake and biological activity of antifungals encapsulated in nanoparticle based vectors. *Sci. Rep.* **2022**, *12*, 7989, doi:10.1038/s41598-022-11533-w.
3. Salgado, M.; Rodríguez-Rojo, S.; Alves-Santos, F.M.; Cocero, M.J. Encapsulation of resveratrol on lecithin and β-glucans to enhance its action against *Botrytis cinerea*. *J. Food Eng.* **2015**, *165*, 13-21, doi:10.1016/j.jfoodeng.2015.05.002.
4. Canales, D.; Montoille, L.; Rivas, L.M.; Ortiz, J.A.; Yañez-S, M.; Rabagliati, F.M.; Ulloa, M.T.; Alvarez, E.; Zapata, P.A. Fungicides films of low-density polyethylene (LDPE)/inclusion complexes (carvacrol and cinnamaldehyde) against *Botrytis cinerea*. *Coatings* **2019**, *9*, 795, doi:10.3390/coatings9120795.
5. Vega-Vásquez, P.; Mosier, N.S.; Irudayaraj, J. Nanovaccine for plants from organic waste: D-limonene-loaded chitosan nanocarriers protect plants against *Botrytis cinerea*. *ACS Sustainable Chemistry & Engineering* **2021**, *9*, 9903-9914, doi:10.1021/acssuschemeng.1c02818.
6. Wang, C.Y.; Jia, C.; Zhang, M.Z.; Yang, S.; Qin, J.C.; Yang, Y.W. A lesion microenvironment-responsive fungicide nanoplatform for crop disease prevention and control. *Advanced Healthcare Materials* **2022**, *11*, 2102617, doi:10.1002/adhm.202102617.
7. Xue, Y.; Zhou, S.; Fan, C.; Du, Q.; Jin, P. Enhanced antifungal activities of eugenol-entrapped casein nanoparticles against anthracnose in postharvest fruits. *Nanomaterials* **2019**, *9*, 1777, doi:10.3390/nano9121777.
8. Tryfon, P.; Kamou, N.N.; Pavlou, A.; Mourdikoudis, S.; Menkissoglu-Spiroudi, U.; Dendrinou-Samara, C. Nanocapsules of ZnO nanorods and geraniol as a novel mean for the effective control of *Botrytis cinerea* in tomato and cucumber plants. *Plants* **2023**, *12*, 1074, doi:10.3390/plants12051074.
9. Hadidi, M.; Motamedzadegan, A.; Jelyani, A.Z.; Khashadeh, S. Nanoencapsulation of hyssop essential oil in chitosan-pea protein isolate nano-complex. *LWT* **2021**, *144*, 111254, doi:10.1016/j.lwt.2021.111254.
10. Hesami, G.; Darvishi, S.; Zarei, M.; Hadidi, M. Fabrication of chitosan nanoparticles incorporated with *Pistacia atlantica* subsp. *kurdica* hulls' essential oil as a potential antifungal preservative against strawberry grey mould. *Int. J. Food Sci. Technol.* **2021**, *56*, 4215-4223, doi:10.1111/ijfs.15110.
11. Erarslan, A.; Karakas, C.Y.; Bozkurt, F.; Sagdic, O. Enhanced antifungal activity of electrosprayed poly (vinyl alcohol)/chitosan nanospheres loaded with sage essential oil on the viability of *Aspergillus niger* and *Botrytis cinerea*. *ChemistrySelect* **2023**, *8*, e202300296, doi:10.1002/slct.202300296.
12. Mohammadi, A.; Hashemi, M.; Hosseini, S.M. Nanoencapsulation of *Zataria multiflora* essential oil preparation and characterization with enhanced *antifungal activity for controlling Botrytis cinerea*, the causal agent of gray mould disease. *Innovative Food Science & Emerging Technologies* **2015**, *28*, 73-80, doi:10.1016/j.ifset.2014.12.011.
13. Seglie, L.; Spadaro, D.; Trotta, F.; Devecchi, M.; Gullino, M.L.; Scariot, V. Use of 1-methylcylopropene in cyclodextrin-based nanosponges to control grey mould caused by *Botrytis cinerea* on *Dianthus caryophyllus* cut flowers. *Postharvest Biology and Technology* **2012**, *64*, 55-57, doi:10.1016/j.postharvbio.2011.09.014.
14. Raj, V.; Raorane, C.J.; Lee, J.-H.; Lee, J. Appraisal of chitosan-gum arabic-coated bipolymeric nanocarriers for efficient dye removal and eradication of the plant pathogen *Botrytis cinerea*. *ACS Applied Materials & Interfaces* **2021**, *13*, 47354-47370, doi:10.1021/acsami.1c12617.
15. Zhang, X.; Tang, X.; Zhao, C.; Yuan, Z.; Zhang, D.; Zhao, H.; Yang, N.; Guo, K.; He, Y.; He, Y.; Hu, J.; He, L.; He, L.; Qian, K. A pH-responsive MOF for site-specific delivery of fungicide to control citrus disease of *Botrytis cinerea*. *Chem. Eng. J.* **2022**, *431*, 133351, doi:10.1016/j.cej.2021.133351.
16. Ren, L.; Zhao, J.; Li, W.; Li, Q.; Zhang, D.; Fang, W.; Yan, D.; Li, Y.; Wang, Q.; Jin, X.; Cao, A. Site-specific controlled-release imidazolate framework-8 for dazomet smart delivery to improve the effective utilization rate and reduce biotoxicity. *J. Agric. Food. Chem.* **2022**, *70*, 5993-6005, doi:10.1021/acs.jafc.2c00353.
17. Tang, G.; Tian, Y.; Niu, J.; Tang, J.; Yang, J.; Gao, Y.; Chen, X.; Li, X.; Wang, H.; Cao, Y. Development of carrier-free self-assembled nanoparticles based on fenhexamid and polyhexamethylene biguanide for sustainable plant disease management. *Green Chemistry* **2021**, *23*, 2531-2540, doi:10.1039/d1gc00006c.

18. Sharma, S.; Singh, B.; Bindra, P.; Panneerselvam, P.; Dwivedi, N.; Senapati, A.; Adholeya, A.; Shanmugam, V. Triple-smart eco-friendly chili anthracnose control agro-nanocarrier. *ACS Applied Materials & Interfaces* **2021**, *13*, 9143-9155, doi:10.1021/acsami.0c18797.
19. Niu, X.; Lin, L.; Liu, L.; Wang, H. Preparation of a novel glucose oxidase-N-succinyl chitosan nanospheres and its antifungal mechanism of action against *Colletotrichum gloeosporioides*. *Int. J. Biol. Macromol.* **2023**, *228*, 681-691, doi:10.1016/j.ijbiomac.2022.12.171.
20. Tofiño-Rivera, A.P.; Castro-Amaris, G.; Casierra-Posada, F. Effectiveness of *Cymbopogon citratus* oil encapsulated in chitosan on *Colletotrichum gloeosporioides* isolated from *Capsicum annuum*. *Molecules* **2020**, *25*, 4447, doi:10.3390/molecules25194447.
21. Gundewadi, G.; Rudra, S.G.; Gogoi, R.; Banerjee, T.; Singh, S.K.; Dhakate, S.; Gupta, A. Electrospun essential oil encapsulated nanofibers for the management of anthracnose disease in sapota. *Ind. Crops Prod.* **2021**, *170*, 113727, doi:10.1016/j.indcrop.2021.113727.
22. Liang, W.; Zhang, J.; Wurm, F.R.; Wang, R.; Cheng, J.; Xie, Z.; Li, X.; Zhao, J. Lignin-based non-crosslinked nanocarriers: A promising delivery system of pesticide for development of sustainable agriculture. *Int. J. Biol. Macromol.* **2022**, *220*, 472-481, doi:10.1016/j.ijbiomac.2022.08.103.
23. Xu, L.; Cao, L.-D.; Li, F.-M.; Wang, X.-J.; Huang, Q.-L. Utilization of chitosan-lactide copolymer nanoparticles as controlled release pesticide carrier for pyraclostrobin against *Colletotrichum gossypii* Southw. *J. Dispersion Sci. Technol.* **2014**, *35*, 544-550, doi:10.1080/01932691.2013.800455.
24. Yao, J.; Cui, B.; Zhao, X.; Zhi, H.; Zeng, Z.; Wang, Y.; Sun, C.; Liu, G.; Gao, J.; Cui, H. Antagonistic effect of azoxystrobin poly (lactic acid) microspheres with controllable particle size on *Colletotrichum higginsianum* Sacc. *Nanomaterials* **2018**, *8*, 857, doi:10.3390/nano8100857.
25. Weisany, W.; Samadi, S.; Amini, J.; Hossaini, S.; Yousefi, S.; Maggi, F. Enhancement of the antifungal activity of thyme and dill essential oils against *Colletotrichum nymphaeae* by nano-encapsulation with copper NPs. *Ind. Crops Prod.* **2019**, *132*, 213-225, doi:10.1016/j.indcrop.2019.02.031.
26. Xu, X.; Peng, X.; Huan, C.; Chen, J.; Meng, Y.; Fang, S. Development of natamycin-loaded zein-casein composite nanoparticles by a pH-driven method and application to postharvest fungal control on peach against *Monilinia fructicola*. *Food Chem.* **2023**, *404*, 134659, doi:10.1016/j.foodchem.2022.134659.
27. de Castro e Silva, P.; Pereira, L.A.S.; de Rezende, É.M.; dos Reis, M.V.; Lago, A.M.T.; Carvalho, G.R.; Paiva, R.; Oliveira, J.E.; Marconcini, J.M. Production and efficacy of neem nanoemulsion in the control of *Aspergillus flavus* and *Penicillium citrinum* in soybean seeds. *Eur. J. Plant Pathol.* **2019**, *155*, 1105-1116, doi:10.1007/s10658-019-01838-4.
28. Prasad, J.; Das, S.; Maurya, A.; Jain, S.K.; Dwivedy, A.K. Synthesis, characterization and in situ bioefficacy evaluation of *Cymbopogon nardus* essential oil impregnated chitosan nanoemulsion against fungal infestation and aflatoxin B1 contamination in food system. *Int. J. Biol. Macromol.* **2022**, *205*, 240-252, doi:10.1016/j.ijbiomac.2022.02.060.
29. Das, S.; Singh, V.K.; Dwivedy, A.K.; Chaudhari, A.K.; Upadhyay, N.; Singh, P.; Sharma, S.; Dubey, N.K. Encapsulation in chitosan-based nanomatrix as an efficient green technology to boost the antimicrobial, antioxidant and in situ efficacy of *Coriandrum sativum* essential oil. *Int. J. Biol. Macromol.* **2019**, *133*, 294-305, doi:10.1016/j.ijbiomac.2019.04.070.
30. Bhawana; Basniwal, R.K.; Buttar, H.S.; Jain, V.K.; Jain, N. Curcumin nanoparticles: Preparation, characterization, and antimicrobial study. *J. Agric. Food. Chem.* **2011**, *59*, 2056-2061, doi:10.1021/jf104402t.
31. Soltanzadeh, M.; Peighambardoust, S.H.; Ghanbarzadeh, B.; Mohammadi, M.; Lorenzo, J.M. Chitosan nanoparticles encapsulating lemongrass (*Cymbopogon commutatus*) essential oil: Physicochemical, structural, antimicrobial and in-vitro release properties. *Int. J. Biol. Macromol.* **2021**, *192*, 1084-1097, doi:10.1016/j.ijbiomac.2021.10.070.
32. Raimond, L.; Halbus, A.F.; Athab, Z.H.; Paunov, V.N. Antimould action of Ziram and IPBC loaded in functionalised nanogels against *Aspergillus niger* and *Penicillium chrysogenum*. *Materials Advances* **2022**, *3*, 8178-8192, doi:10.1039/d2ma00271j.
33. Liang, Y.; Fan, C.; Dong, H.; Zhang, W.; Tang, G.; Yang, J.; Jiang, N.; Cao, Y. Preparation of MSNs-chitosan@prochloraz nanoparticles for reducing toxicity and improving release properties of prochloraz. *ACS Sustainable Chemistry & Engineering* **2018**, *6*, 10211-10220, doi:10.1021/acssuschemeng.8b01511.
34. Hong, T.; Wan, M.; Lv, S.; Peng, L.; Zhao, Y. Metal-phenolic coated rod-like silica nanocarriers with pH responsiveness for pesticide delivery. *Colloids and Surfaces A: Physicochemical and Engineering Aspects* **2023**, *662*, 130989, doi:10.1016/j.colsurfa.2023.130989.
35. Huang, Y.; Yang, Y.; Liang, B.; Lu, S.; Yuan, X.; Jia, Z.; Liu, J.; Liu, Y. Green nanopesticide: pH-responsive eco-friendly pillar[5]arene-modified selenium nanoparticles for smart delivery of

carbendazim to suppress *Sclerotinia* diseases. *ACS Applied Materials & Interfaces* **2023**, *15*, 16448-16459, doi:10.1021/acsami.2c23241.
36. Gao, Y.; Liang, Y.; Dong, H.; Niu, J.; Tang, J.; Yang, J.; Tang, G.; Zhou, Z.; Tang, R.; Shi, X.; Cao, Y. A bioresponsive system based on mesoporous organosilica nanoparticles for smart delivery of fungicide in response to pathogen presence. *ACS Sustainable Chemistry & Engineering* **2020**, *8*, 5716-5723, doi:10.1021/acssuschemeng.0c00649.
37. Xiao, D.; Cheng, J.; Liang, W.; Sun, L.; Zhao, J. Metal-phenolic coated and prochloraz-loaded calcium carbonate carriers with pH responsiveness for environmentally-safe fungicide delivery. *Chem. Eng. J.* **2021**, *418*, 129274, doi:10.1016/j.cej.2021.129274.
38. Shi, L.; Liang, Q.; Zang, Q.; Lv, Z.; Meng, X.; Feng, J. Construction of prochloraz-loaded hollow mesoporous silica nanoparticles coated with metal–phenolic networks for precise release and improved biosafety of pesticides. *Nanomaterials* **2022**, *12*, 2885, doi:10.3390/nano12162885.
39. Yang, J.; Gao, Y.; Zhou, Z.; Tang, J.; Tang, G.; Niu, J.; Chen, X.; Tian, Y.; Li, Y.; Cao, Y. A simple and green preparation process for PRO@PIL-PHS-PEC microcapsules by using phosphonium ionic liquid as a multifunctional additive. *Chem. Eng. J.* **2021**, *424*, 130371, doi:10.1016/j.cej.2021.130371.
40. Liang, W.; Xie, Z.; Cheng, J.; Xiao, D.; Xiong, Q.; Wang, Q.; Zhao, J.; Gui, W. A light-triggered pH-responsive metal–organic framework for smart delivery of fungicide to control *Sclerotinia* diseases of oilseed rape. *ACS Nano* **2021**, *15*, 6987-6997, doi:10.1021/acsnano.0c10877.
41. Peng, F.; Wang, X.; Zhang, W.; Shi, X.; Cheng, C.; Hou, W.; Lin, X.; Xiao, X.; Li, J. Nanopesticide formulation from pyraclostrobin and graphene oxide as a nanocarrier and application in controlling plant fungal pathogens. *Nanomaterials* **2022**, *12*, 1112, doi:10.3390/nano12071112.